Fiber Optical Micro-detectors for Oxygen Sensing in Power Plants

Quarterly Technical Report
Reporting Period:
April 1, 2005 to June 30, 2005

Gregory L. Baker*, Ruby N. Ghosh[+], D.J. Osborn III*, Po Zhang[+]

July 2005

DOE Award Number: DE-FC26-02NT41582

*536 Chemistry Building, Department of Chemistry
[+]2170 BPS, Center for Sensor Materials and Dept. of Physics
Michigan State University

DISCLAIMER

ABSTRACT

A reflection mode fiber optic oxygen sensor is being developed that can operate at high temperatures for power plant applications. The sensor is based on the $^3O_2$ quenching of the red emission from hexanuclear molybdenum chloride clusters. Two critical materials issues are the cluster's ability to withstand high temperatures when immobilized in a porous the sol-gel support, and whether after heating to high temperatures, the sol-gel matrix maintains a high and constant permeability to oxygen to support rapid quenching of luminescence. We used a composite materials approach to prepare stable sensing layers on optical fibers. We dispersed 60 w/w% of a pre-cured sol-gel composite containing the potassium salt of molybdenum clusters ($K_2Mo_6Cl_{14}$) into a sol-gel binder solution, and established the conditions necessary for deposition of sol-gel films on optical fibers and planar substrates. The fiber sensor has an output signal of 5 nW when pumped with an inexpensive commercial 365 nm ultraviolet light emitting diode (LED). Quenching of the sensor signal by oxygen was observed up to a gas temperature of 175 °C with no degradation of the oxygen permeability of the composite after high temperature cycling. On planar substrates the cluster containing composite responds within <1 second to a gas exchange from nitrogen to oxygen, indicating the feasibility of real-time oxygen detection.

TABLE OF CONTENTS

LISTS OF GRAPHICAL MATERIAL

INTRODUCTION

Maximizing the efficiency of the combustion process requires real-time control of the correct fuel/oxygen ratio. This requires the ability to sense oxygen levels over a broad range of concentrations with fast response times. Mussell, Newsham, and Ruud previously reported preliminary studies of the synthesis and optical properties of Mo_6Cl_{12}-based clusters relevant to this project.[1-4] Mussell described the synthesis of the molybdenum clusters, and Newsham gives a good account of the properties of neutral Mo_6Cl_{12} clusters and their salts, in both solution and a sol gel matrix. Newsham's data indicate that the photophysical properties of the clusters are maintained in sol gel matrices. To prepare a fiber optic sensor based on Mo_6Cl_{12}, Ruud dispersed Mo_6Cl_{12} in poly[1-trimethylsilyl-1-propyne] (PTMSP), and used a dipping technique to immobilize the composite at the cleaved end of a silica optical fiber. Ghosh and co-workers [5] demonstrated a fast room temperature fiber optic sensor based on oxygen quenching of the luminescence from the PTMSP/Mo_6Cl_{12} composites. While the PTMSP support is adequate for room temperature applications, is unable to withstand the high temperatures associated with combustion in a power plant. To improve the sensor's high temperature performance, we are replacing PTMSP with a thermally stable sol gel matrix that should be able to withstand the higher temperature requirements of the power plant combustion process. The idea of using a sol gel as the support matrix for high temperature oxygen sensor application is not new. Remillard and coworkers have shown that a sol gel supported copper based oxygen sensor can be used in a combustion process.[6] With these facts in hand, we anticipate promising results from our design.

EXECUTIVE SUMMARY

A requirement of optical sensors based on luminescence quenching is that the lumophore have a strong luminescence that is efficiently quenched by oxygen, and that oxygen has ready access to the lumophore. For a high temperature sensor, these characteristics must hold over the entire temperature range of interest.

Previously we investigated dip and spray coating approaches for immobilizing clusters on planar substrates and the tips of high-temperature optical fibers. A comparison of the resulting film thicknesses with the optical characteristics of high-temperature fibers suggested that the sol-gel films needed to be substantially thicker than can be easily obtained by either method. Our proposed solution was to modify the sol-gel solution and spray coat the tips of fibers with a slurry of cured $K_2Mo_6Cl_{14}$/sol-gel nanoparticles in a sol-gel solution. Slurries with varying weight fractions of cluster-containing particles in a pure sol-gel binder were prepared. The sensors fabricated for this report show increased thickness, adhesion, and the required lumophore concentration for an optical fiber based oxygen sensor.

A synthetic challenge is to increase the quenching ratio to four or better. Adding nanoparticulate fumed silica to the sol-gel preparations initially improved the quenching ratio but did not improve the long-term stability of quenching at 200 °C. To improve the long-term stability at 200 °C, sensors were prepared by coating optical fibers with 50 and 60 w/w% blends resulting in a more uniform coating, enhanced oxygen quenching, and improved adhesion. Our 3rd quarter milestone was to: "Complete immobilization of alkali metal salt derivatives of Mo_6Cl_{12} at the tip of a high temperature silica optical fiber.

We have designed and built a compact high temperature fiber sensor test setup to characterize devices up to 350 °C in a gas flow through system. The setup is designed to be portable for field testing and uses an inexpensive, ~$6.00 UV light emitting diode as the excitation source. A data acquisition system has been developed to simultaneously record the sensor luminescence signal and sensor temperature, to ±1 °C. We expect to be able to determine the sensor response time to better than 10 s, as the gas exchange time in the chamber is <6 s for a 1.5 L/min flow.

The luminescence signal from a fiber sensor (Fiber D) fabricated using the composite approach of embedding cured $K_2Mo_6Cl_{14}$/sol-gel nanoparticles in an optically inert sol-gel binder was measured from room temperature to 175 °C. Quenching ratios (signal in pure N_2 vs 21% O_2) of 2.4X and 1.3X were obtained at 115 and 175 °C respectively. The signal to noise ratio for the 115 °C measurement is ~4dB in oxygen. We are in the process of reducing the background light level of our present setup below 0.22 nW to improve our sensitivity. An exciting result of our fiber measurements is that the thick 200 μm cluster containing sensing film, displays a stronger degree of luminescence quenching by oxygen after high temperature cycling than any of our previous films. This indicates that the composite retains its oxygen permeability following thermal cycling. These sensing measurements were made on a prototype device fabricated on an inexpensive UV transparent optical fiber designed for medium temperature operation, we

are currently in the process of fabricating devices on the 200 °C Fiber Guide and 400 °C Cerampoptic fibers identified in the previous reporting period.

In addition to the fiber sensor experiments we performed *in-situ* measurements of the emission spectra of a composite film deposited on a planar substrate (Film 38Q) up to 200 °C. This is the first high temperature data we have been able to obtain that is free of fluorescence generated by the heating structure itself. The spectra show that the emission line shape remains relatively constant as a function of temperature. By monitoring the emission intensity as a function of time, while alternating between pure nitrogen and 21% oxygen, we find a quenching ratio of about 1.3X at 200 °C. The response time of this film is remarkable fast <2.5 s at 175 °C. The sensor signal switches between two discrete levels, without any of the long term exponential tails observed in our previous sol-gel films.

Our paper entitled "Mo_6Cl_{12}-Incorporated Sol-Gel for Oxygen Sensing Applications" by D.J. Osborn III, Gregory L. Baker and Ruby N. Ghosh," has been accepted for publication in the Journal of Sol-Gel Science and Technology.

EXPERIMENTAL

Materials.

All glassware was oven-dried prior to use. Acetonitrile (Spectrum Chemical Company, HPLC grade) was dried over CaH_2 and distilled prior to use. Tetraethyl orthosilicate (TEOS) (Aldrich, 98%) and hydrochloric acid (CCI, electronics grade) were used as received. Corning 7980 quartz microscope slides (3" × 1" × 1 mm) were obtained from Technical Glass Products and cut into 1.25 cm × 2.45 cm pieces. Slides were handled with gloves and tweezers in order to minimize surface contamination.

MM5 and MM8 $K_2Mo_6Cl_{14}$ Clusters.

The synthesis and characterization of MM5 and MM8 is described in our previous two reports. For sol-gel/cluster composite 31 the luminescent cluster source is MM5, while for slide 38Q, the MM8 generation of clusters was used. Thermogravimetric analyses of MM5 and MM8 indicate that the MM8's thermal stability is slightly better. Since MM5 was the source of the clusters used in the composite powder binder for slide 38Q and the optical fibers described in this report, high temperature data from these materials should be considered to be the minimum expected for sensors prepared from MM8.

Stock sol-gel solutions for binders.

A typical stock sol-gel solution for the coating process was prepared as described below. TEOS (100 mL, 0.477 mol) and acetonitrile (70.3 mL) were added to a 500 mL Erlenmeyer flask. With stirring, water (32.3 mL, adjusted to pH=1 with HCl) was added and the solution was stirred for 1 hour at room temperature. The stir bar was removed from the flask and the solution was heated in an oil bath at 70 ºC for 2.5 hours. The solution was then transferred to a 500 mL glass bottle, capped, and aged at room temperature until use.

Composite powder / sol-gel binder blend.

A previously prepared cluster-containing sol-gel solution (composite 31) was aged at room temperature for 4 months in a sealed vial to obtain a solid monolith. The monolith was then ground by hand to a powder with particle sizes ranging from 25 – 250 μm using a mortar and pestle. The powder was then cured for 24 hours at 70 ºC to drive the sol-gel reactions toward completion. Blends of 30, 50, 60, and 80 w/w% were prepared by adding a known mass of stock sol-gel solution to a predetermined mass of the composite 31 powder to obtain a light yellow suspension that was then mixed with gentle grinding in a small vial to maximize homogeneity.

A control for fiber sensor analysis was prepared from a stock sol-gel solution without added cluster (composite 21). After aging at room temperature for 4 months in a sealed vial, the solid monolith was ground using a mortar and pestle to a powder with particle sizes ranging from 25 – 250 μm. The powder was cured for 24 hours at 70 ºC to drive the sol-gel reactions toward completion and then was pulverized for 15 minutes in a Wig-L-Bug (a small ball mill) to obtain a white powder with 1 – 2 μm diameter particles. The

powder also was used to assess the film quality that can be obtained from <10 μm particulates.

Dip coating.
Fibers were cleaned by mechanically removing 1 cm of jacket and cladding to expose the fiber core. The fiber core was wiped using an acetone-soaked Kimwipe to remove residual cladding material, rinsed with deionized water, and placed into a 2M KOH solution for 20 minutes to hydroxylate the surface for maximum adhesion. The fibers were removed from the KOH solution and rinsed with10 mL of deionized water, and re-dipped into 2 M KOH to test wetting. If necessary, the KOH treatment, water rinse, and wetting test were repeated until the KOH solution wet the fiber surface. Once wetting was satisfactory, the fiber tip was rinsed with 10 mL of deionized water and dried using a stream of nitrogen gas. The fibers were immediately dipped into a 50 w/w% (fiber E) or 60 w/w% (fibers C, D, and H) composite powder / sol-gel solution blend.

Fibers were dipped by hand at a 15º angle for better coating of tip and allowed to dry vertically for one hour under ambient conditions to maximize coating uniformity on the tip. Fibers were cured at 70 ºC for times ranging from 4 to 12 hours. Specifically, fiber C was cured for 1 hour at 23 ºC, fiber D was cured for 12 hours at 70 ºC, fiber E was cured for 10 hours at 70 ºC, and fiber H was cured for 8 hours at 70 ºC.

Spray coating – planar sample 38Q.
For sample 38Q, 25.9 mg of $K_2Mo_6Cl_{14}{\cdot}2H_2O$ was added to 10 mL of 10-day old stock sol-gel solution. After stirring overnight, 35.9 mg of composite 31 (25 – 250 μm diameter particles) was added and stirred for 24 hours to form a cloudy suspension. Once stirring ceased, ~25% of the particulates remained suspended.

Following the procedure described by Remillard et al., [6] a pulverized composite 31 / sol-gel solution blend was placed into a 20 mL vial and attached to a Paasche double-action internal-mix airbrush. A single coat was applied to a 2.4 cm × 1.25 cm quartz slide for 1 second at a distance of 4 cm from the airbrush tip using nitrogen gas at 10 psi. Immediately after coating the sample, it was placed into an oven and cured for 30 minutes in air at 200 ºC.

Mechanical testing of composite adhesion.
The mechanical properties of all fibers were evaluated by first gently tapping on the edge of the bench top, dropped from a height of one meter, and then followed by application of Scotch brand adhesive tape. Fibers C and D withstood tapping on the edge of the bench top and showed minor loss of coating when dropped from a height of one meter. Fibers C and D did not pass the more rigorous adhesive tape test.

Optical microscopy of thin films and fibers.
Optical microscopy images were acquired using a Nikon Optiphot2-Pol equipped with a Sony Hyper HAD CCD-IRIS/RGB color video camera (model DXC-151A). The camera was connected to a PC using a Sony camera adapter (model CMA-D2). The images were

viewed using a Sony Trinitron color video monitor. Images were taken using Hauppage computer works Win/TV software (version 2.4.17052).

Dark field images

Dark field optics is a low cost alternative to phase contract microscopy that allows one to readily obtain information on surface topography. In dark field the sample is illuminated from above, and only photons collected by annular apertures are collected to form the image. A perfectly flat sample with no topography will appear dark, any topographic features will be accentuated in the image. We used an Olympus BX60 optical microscope in KMF clean room, with 10X, 20X, 50X and 100X dark filed objectives and a SPOT video camera (Diagnostic Instrument model 1.3.0) with imageGear version 6.6.4 software. The particle size of sol-gel powders prepared using the small ball mill (Wig-L-Bug). The individual particles are ~5 μm, with larger 50 μm aggregates.

Absorption spectroscopy.

Samples were prepared by weighing 2 - 3 mg of Mo_6Cl_{12} in a small sample vial. The compound was then dissolved in a small amount of dry acetonitrile and transferred to a 10 mL volumetric flask. The volumetric flask was filled to the mark, stoppered, and shaken to insure a homogenous solution. Typical concentrations were 1.7×10^{-4} M. Absorption spectra were measured using a Perkin-Elmer Lambda 40 series double beam UV/vis spectrometer. Data analysis was performed using the UV Win lab (version 2.80.03) software package supplied with the instrument and plotted using Microsoft Excel. Solutions were placed into a 1 cm pathlength quartz cuvette with a separate cell containing only solvent as a reference.

Fluorescence spectroscopy.

The fluorescence measurements were performed using a Fluorolog-3 instrument from Instruments S.A., Inc. The system includes a single Czerny-Turner excitation spectrometer with a 1200 g/mm ruled grating blazed at 330 nm and a single Czerny-Turner emission spectrometer with a 1200 g/mm holographic grating blazed at 630 nm. The excitation optics consists of a 450W ozone free Xe lamp, followed by a 270-380 nm bandpass filter (Oriel 1124). A Si photodiode is used to continuously monitor the lamp signal. The detection optics consists of 603.2 nm long wave pass filter (CVI) followed by a multi-alkali photo multiplier tube (Hamamatsu R928) with photon counting electronics. Data processing was performed using the Datamax (version 2.2) software package supplied with the instrument. Spectra were obtained by exciting at 313 nm and scanning the emission monochromator from 550 to 850 nm.

The measurements of the $K_2Mo_6Cl_{14}$ emission from Mo-cluster / sol-gel composite films were made in the quartz cuvette sealed with an airtight septum. Nitrogen gas with purity 99.999% was used to obtain the luminescence spectra in a non-oxygen environment. The oxygen measurements (21% oxygen in nitrogen) were performed using 99.999% purity gas. The nitrogen and oxygen were injected via a needle passing through the septum and allowing the gas in the cuvette to equilibrate for 10 min. An external gas flow switch was designed and built to conveniently change the gas environment without needing to touch the spectrometer compartment. This switch allows us to be completely certain that the sample does not move during repeated gas exchange.

High temperature in-situ fluorescence measurements

The *in-situ* measurements of the Mo_6Cl_{12} emission from Mo-cluster / sol-gel composite films as a function of temperature were made in the same quartz cuvette described above. The incident pump beam in the fluorimeter is ~ 2.0 × 10 mm; we use a small platinum microheater (part 32 208 172 from Heraeus Sensor Technology), 2.5 × 9.7 mm in size, to heat only the area under investigation. We previously encountered problems with the silver paint used to attach the heater to the slide as the silver paint itself fluoresces in the visible upon UV irradiation. To circumvent this problem we used silver paint to attach the Pt heater to the unpolished side of a small (15 × 4.5 mm) piece of single crystal Si, which does not fluoresce. Since the polished side of the Si piece and the back side of the quartz slide are optically flat, simply clamping the two pieces together achieves intimate contact without the need for an adhesive. The contact quality can be judged by interference fringes that appear at the interface between the wafer and quartz slide. Because the silica wafer has a high thermal conductivity, uniform heating of the quartz film can be reached quickly and efficiently. The absence of luminescence from this sandwich-like structure was verified by measuring the emission spectrum of an uncoated quartz slide as a function of temperature.

Electrical connection to the Pt heater was made by microwelding 5 mil diameter Cu wire to the 5 mil diameter legs of the Pt microheater. The electrical leads were then threaded through the septum. The microheater was powered with a regulated voltage supply. We determined the heater temperature by monitoring the heater resistance, and using the resistance versus temperature curves for a standard 100Ω Pt thermometer. The thermal impedance R_{total} of the quartz slide was independently determined. Thus, by monitoring the backside heater resistance we know the temperature of the front side of the slide to ±5 °C. Shown in **Figure 1** is a diagram of the structure used for the *in-situ* measurements.

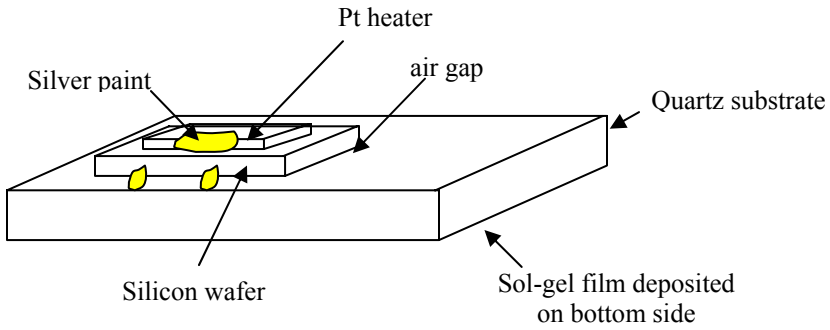

Figure 1. Diagram of the sandwich–like structure used for *in-situ* high temperature measurements of slide 38Q.

The total thermal impedance, R_{total} , is calculated using equation (1)

$$R_{total} = \frac{t_1}{K_{Si}A} + \frac{t_{airgap}}{K_{air}A} + \frac{t_2}{K_{qtz}A_{qtz}} \qquad (1)$$

where *t* represents the thickness of the silicon wafer, quartz substrate and air gap, *K* is thermal conductivity, and *A* is the contact area between the two media of interest

Table 1. Parameters for calculating thermal impedance.

	Quartz	**Wafer**	**Air Gap**
K (Wcm^{-1} K^{-1})	0.0138 (23 °C) 0.0146 (100 °C) 0.0155 (200 °C)	1	0.00024
t (mm)	1	0.507	0.01
A (mm^2)	312.5	67.5	67.5

R_{total}= 8.5174 K/W, W=VI, where V is the applied heater voltage and I is the measured heater current.

Sensor data acquisition and measurement

For real time applications, we need a technique to monitor the signal from the fiber optic sensor as a function of both temperature and time. With Mr. Nate Vehanovitz (Troy Inc.), we developed a Labview program for sensor data acquisition and temperature monitoring. The hardware requirements are a laptop running Windows XP or 2000 equipped with a PCMCIA-GBIP card from National Instruments, a GPIB cable, a Keithley digital multimeter and Fluke 45 voltmeter (**Figure2).** During fiber sensor measurements, the Keithley voltmeter monitors the sensor voltage signal (which is proportional to the luminescence intensity) while the Fluke digital multimeter (DMM) monitors the temperature output from a k-type thermocouple and 80TK readout module. The front panel of the data acquisition program is shown in **Figure 3**.

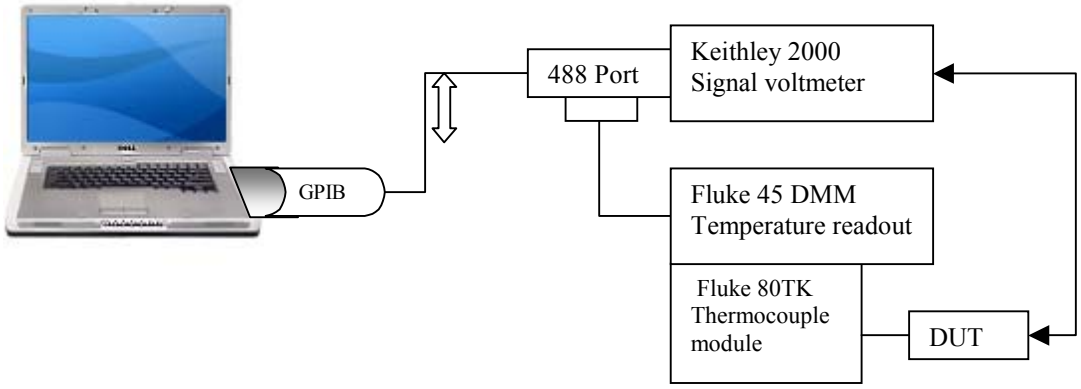

***Figure 2*:** Block diagram of the sensor and temperature data acquisition system.

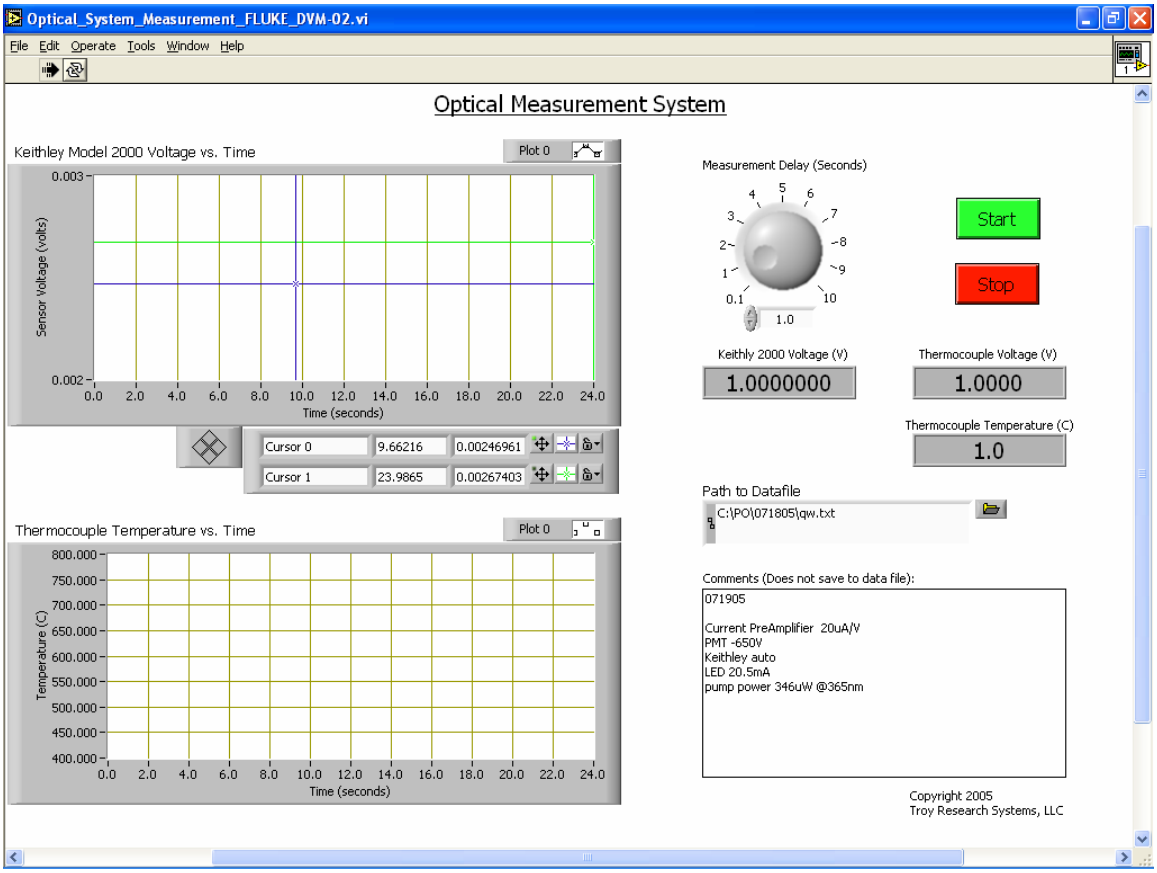

Figure 3: User interface of the automated optical sensor data acquisition software OMS_02.exe.

The data are displayed on an oscilloscope-like screen during real time measurements (see **Figure 3**). The user can save data to a specified data-file after popping out a *Save As* window. The user can also write down experimental condition in comments window and set a continual sampling rate by adjusting a knob on right-up window. Two plotting windows on the left display record the sensor signal and temperature, respectively. The cursors can be moved during the course of the measurement to provide real-time output of signal amplitude and time. The program generates one data file (.txt) with the output data in tab-separated columns.

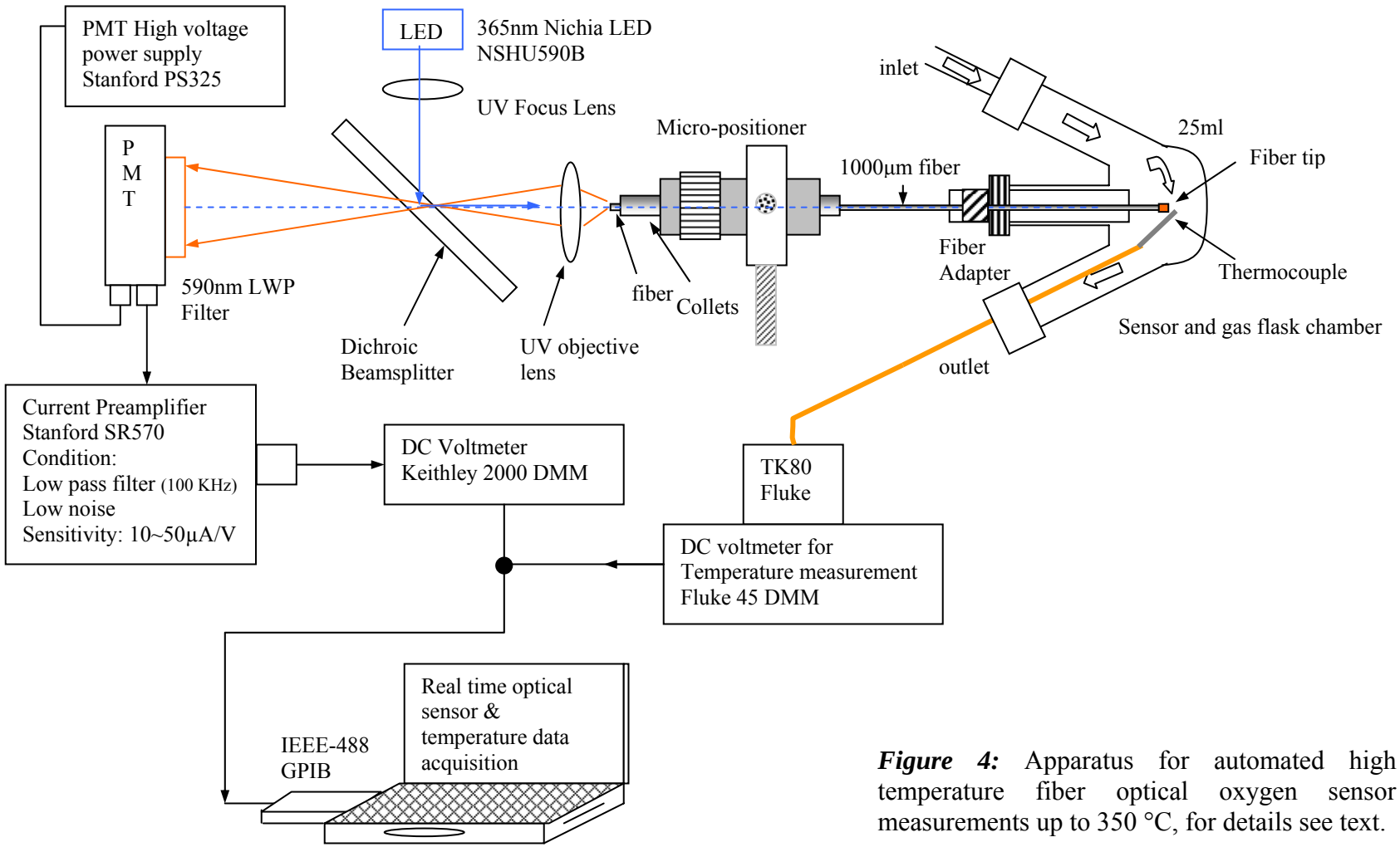

Figure 4: Apparatus for automated high temperature fiber optical oxygen sensor measurements up to 350 °C, for details see text.

High temperature fiber optical sensor measurement system

We designed a setup for automated high temperature reflection-mode fiber optic sensor measurements (see **Figure 4**). A low cost ($6.00) 365 nm UV LED from Nichia 365 nm provides 500 μW of pump power, which is coupled into the fiber via a UV lens (20mm focal length at 360 nm) and a micro-positioner for 3D fiber adjustments at the micron level. A 45° dichroic beam-splitter: separates the pump and signal beams. The 45° transmission ratio is 99.16% at 670 nm and 0.12% at 365 nm. We are able to couple 250 μW of UV light into 1000 μm high temperature fibers. The reflected red luminescence from the fiber tip in the 590 – 900 nm bandwidth, passes through a 590 nm long-wave pass (LWP) filter and is collected with a high sensitivity photomultiplier tube (Hamamatsu R955; gain of 10^6 for an applied bias V_h of –650V, shot noise of 0.3 nA.); one 633 nm photon per second corresponds to a current output of 6.56 pA. A Stanford SR570 preamplifier is used to further amplify the photoelectron current. In the fiber sensor chamber, a heated gas stream (30 – 350 °C) impinges on the fiber sensor tip at a flow rate of 1 – 1.5 L/min. The gas exchange time in the flask is <6s.

The high temperature gas chamber consist of a three-neck round flask, with sensor installation, gas inlet/outlet and thermocouple ports. A 400 ˚C heating tape was wrapped on the outside of the 25 mL flask to obtain a stable high temperature gas stream up to 350 °C with a ± 1 °C variation. A k-type thermocouple (Omega Inc.) was positioned close to the fiber tip to accurately monitor the tip temperature. The temperature value can be directly read on a Fluke voltmeter after transferring the data from the TK80 module (Fluke Inc.). The compact design of our optical system, will allow us to place it inside the sample compartment of the Fluorolog florescence spectrometer for future measurements.

To determine the sensor signal in absolute units we calculate the sensor signal V in nanowatts using the following instrumental parameters:

$$\boldsymbol{P} = S \times V/S_c/G \times 10^6 \ \text{(nW)} \ldots\ldots\ldots\ldots\ldots\ldots (2)$$

V_h,	PMT applied high voltage	(V)
S,	preamplifier sensitivity	(μA/V)
G,	PMT current gain	
S_c,	PMT cathode sensitivity	(41 mA/W@ 633nm)

For typical system parameter values of V_h = –650 V and S =20 μA/V using the PMT specifications from Hamamatsu *Inc*. [7], a 1 volt output signal corresponds to a photon power of 1.023 nW.

A number of measurements were performed to characterize the optical performance of the overall system. First, we evaluated the stray light level of the system. With only the PMT and current preamplifier turned on, we measured a 0.0005 nW signal. Secondly, after turning on the pump LED, but without an optical fiber in the path, the signal increased to 0.13 – 0.15 nW, which sets an upper bound on the *smallest* sensor signal we

could detect. As the UV rejection ratio of the 590 nm LWP filter in front of the PMT is very high, essentially none of the pump signal can be scattered back into the detector, so the 0.15 nW signal must be due to visible fluorescence in the optical path. We are looking into potential sources of this fluorescence, in order to eliminate it. Thirdly, we measured the output signal from bare 1000-µm fibers of various lengths (no cluster on the fiber tip (see **Figure 5**). For a short fibers, an additional 0.07 nW is added due to scattering from the front and back faces of the fiber. The autofluorescence of the fiber itself is low, 2.1×10^{-4} nW/ cm. Later we describe the results for fiber sensor D operating at 100 °C where the signal to noise is ~4 dB in 21% oxygen.

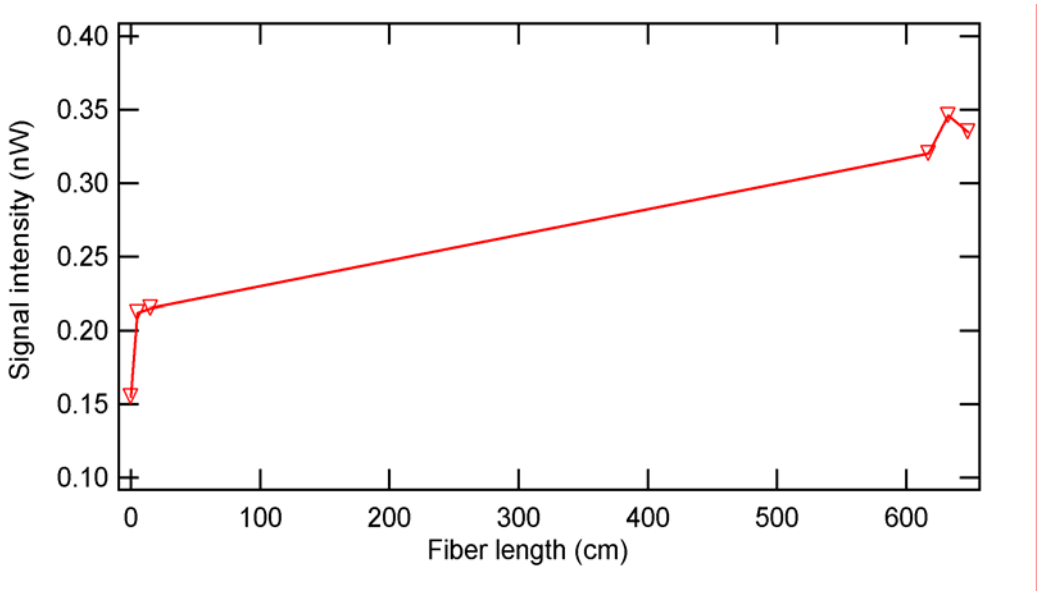

Figure 5: Signal from an uncoated optical fiber as a function of fiber length. The data show low auto-fluorescence (2.1×10^{-4} nW/cm). However, there is a 0.07 nW signal (bandwidth: 590 nm-900 nm) due to reflections off the front and back faces of the fiber

RESULTS AND DISCUSSION

Composite approach to sol-gel matrices containing $K_2Mo_6Cl_{14}$ clusters on fibers and planar substrates.

Our emphasis in the past quarter has been to mobilize molybdenum clusters the end of high-temperature fibers, using methods that ensure high luminescence intensity from the clusters and strong quenching of the luminescence in the presence of oxygen. Previously we discovered that despite long aging and drying times, films deposited on substrates further evolved when they were tested at high temperatures. In general the quenching ratio decreased, which is consistent with densification of the sol-gel matrix. Our hypothesis is that in these materials, the limiting factor in the quenching process is the diffusion of oxygen to the molybdenum clusters, and that the oxygen diffusivity in the heat-treated sol-gel matrices was low. Both the change in the physical parameters of the sol-gel matrix and the low quenching ratio are problems that must be solved in any practical sensor.

As outlined in our last report, we have opted for a composite material approach that involves embedding molybdenum-containing sol-gel particles in a binder that essentially glues the particles to the substrate (**Figure 6**). This approach offers several advantages that will overcome some of the limitations encountered when depositing a homogeneous solution of the cluster in a sol-gel solution. First, by using a preformed and fully equilibrated cluster containing sol-gel matrix, issues related to the long-term aging of the sol-gel matrix are avoided. Second, the use of small particle sizes should lead to large quenching ratios since in the limit of infinitely small particles the diffusivity of oxygen should be dominated by the permeability of the binder. We expect that the binder will be a minority component of the matrix, filling the void space between the particles, and that curing the binder will lead to little if any change in the volume of the composite. The net result is that the binder should have a low density, high oxygen permeability, and that the composite matrix should have an enhanced quenching ratio compared to sol-gel

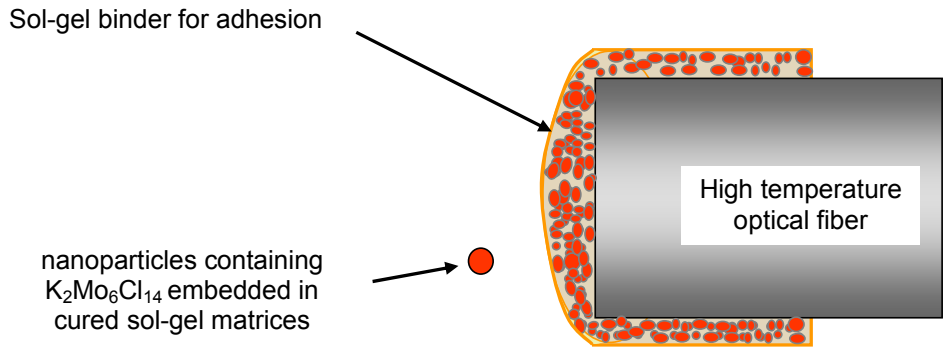

***Figure* 6:** Schematic showing the expected morphology resulting from deposition of a slurry of particles in a sol-gel binder solution. The particles correspond to pre-cured sol-gel particles containing $K_2Mo_6Cl_{14}$ clusters.

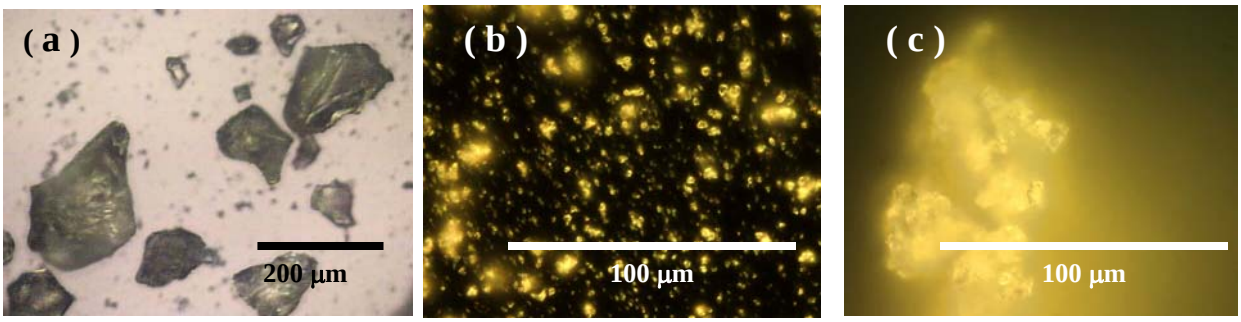

Figure 7: Optical micrographs of sol-gel particles (a) bright field image (10×) showing a sol-gel monolith containing MM5 pulverized using a mortar and pestle, 25 – 250 μm particle size, (b) a sol-gel monolith (no clusters), 1 – 2 μm particle size, and (c) dark field image (100×) showing a sol-gel monolith containing MM5 pulverized via ball milling, 2 – 8 μm particle size.

monoliths. Third, the composite material approach allows us to use the same cluster/sol-gel source for a series of sensors leading to sensors with predictable characteristics.

To that end we selected a monolith previously prepared from a sol-gel solution containing molybdenum clusters (MM5). **Figure 7** shows a micrograph of the MM5 containing sol-gel and the particle size achieved by grinding the monolith into a fine powder using a standard mortar and pestle. A freshly prepared sol-gel solution was added to give a paste-like material composed of either 50 or 60 w/w % particles and the remainder binder. While we eventually plan to use spray-deposition for coating fibers, the viscosity of the paste proved to be too high for effective spraying. Reduction of the particle size seems to be the logical approach for reducing the viscosity since diluting the particles with more sol-gel solution would reduce the net luminescence of the matrix. Coating slides and fibers using a hand-dipping procedure gave films that strongly luminesced. A flow diagram of the composite processing scheme is given in **Figure 9**, with details of the fiber processing schemes and sensor measurements are given in Table **2.** High temperature sensing measurements from fiber D will be described in the next section.

A closer examination of films deposited on fibers (**Figure 8)** shows that the particle sizes are relatively large, between 25 and 150 μm for fibers **C**, **D**, and **E**. As noted above, smaller particles are desired to achieve better quenching ratios and more uniform deposition. Using a ball milling technique reduced the particles to ~5 μm with a significantly tighter size distribution 1-8 μm (see **Figures 7b** and **7c).** The films prepared from these materials are more uniform and smooth, fiber H (**Figure 8).**

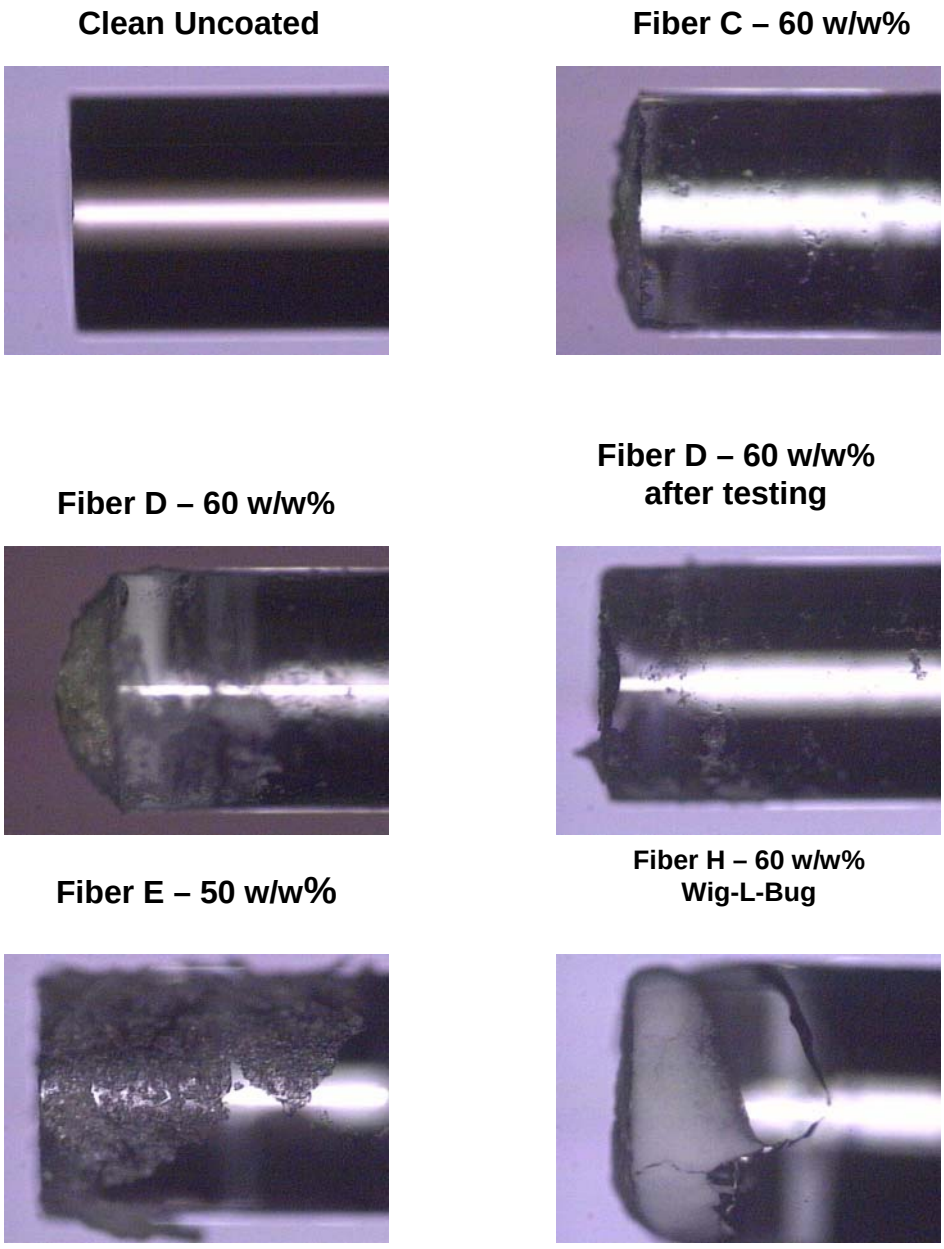

***Figure 8*:** Typical dip coating results for deposition of composite / sol-gel binder blends 1000 μm diameter fibers. Details of the fiber fabrication and resultant measurements are in Table 2.

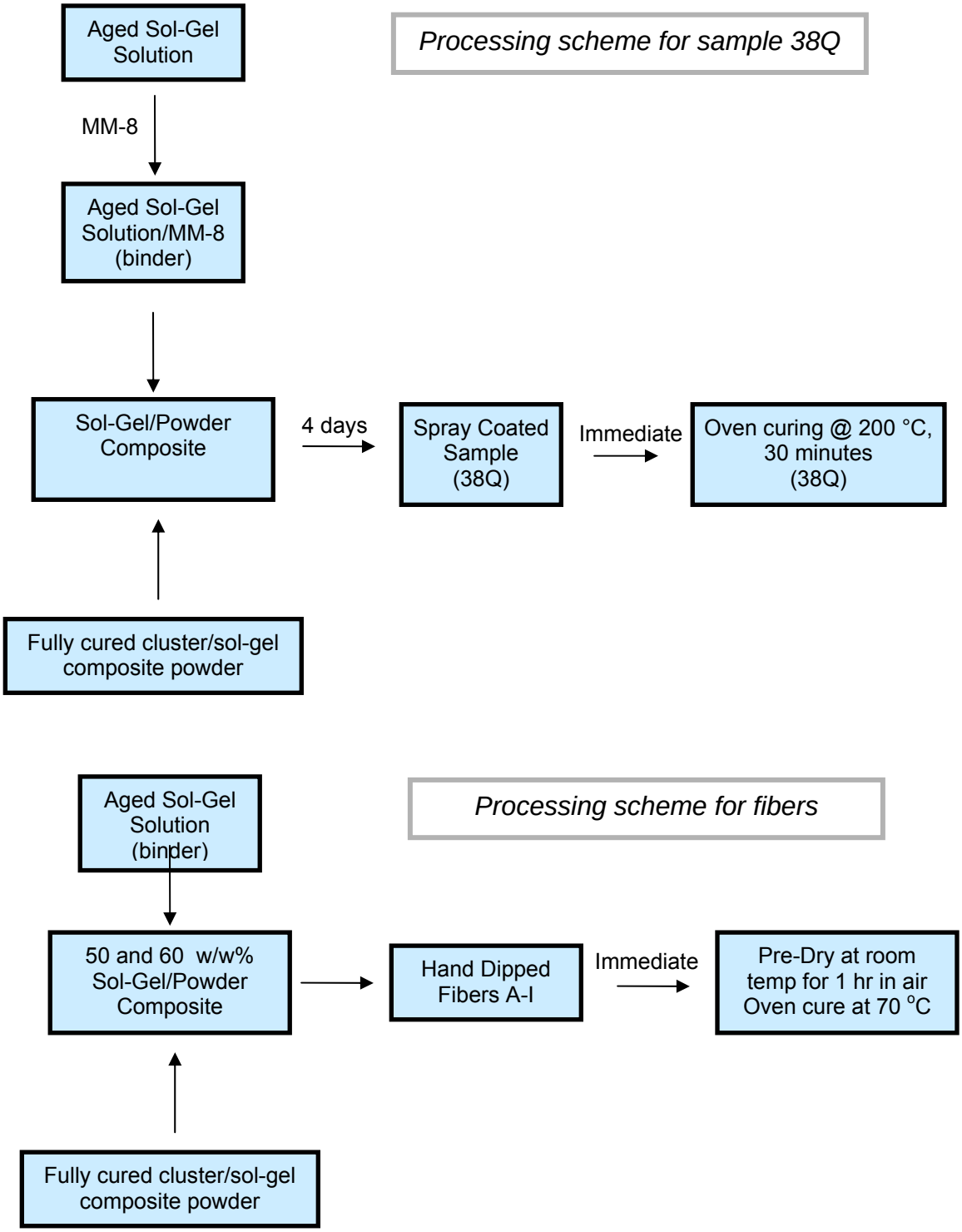

Figure 9: Processing schemes used for fibers and planar sample (slide) 38Q. The principal differences between 38Q and the fibers is that (i) the binder used for 38Q contained molybdenum clusters whereas that for the fibers did not and (ii) 38Q was cured at 200 °C whereas the fibers were cured at 70 °C. The same cluster/sol-gel monolith was used for all samples.

***Table 2*:** Summary of the processing scheme, cluster/sol-gel composite film characteristics and sensing measurements of fibers C, D, E and H (see Figure 7) and slide 38Q (see Figure 13).

	Slide 38Q	**Fiber C**	**Fiber D**	**Fiber E**	**Fiber H**
particle size (μm)	25 – 150	25 – 150	25 – 150	25 – 150	1 – 8
cluster source	MM8	monolith 31 (MM5)	monolith 31 (MM5)	monolith 31 (MM5)	monolith 21
clusters/cm^3	1×10^{20}	4×10^{18}	4×10^{18}	4×10^{18}	No cluster
coating method	spray coat 1×	hand dipped 60 w/w%	hand dipped 60 w/w%	hand dipped 60 w/w%	hand dipped 21 blend 50 w/w%
Coating Date	5/13/2005	6/29/2005	6/30/2005		
Curing Date (Duration, Temp.)	5/13/2005 30min, 200 ºC	6/29/2005 1hr, 23 ºC	6/30/2005 12hr, 70 ºC		
film notes	clear <1μm thick film, thermally cycled 7 hrs	100 μm thick film	200 μm film,		
Quenching ratio (O_2 / N_2)	1.5 at room temp 2.5 – 1.5 after heating	1.3 after heating	>5 at room temp ≥6 after 175 °C	NA	NA
Signal (N_2)	$2.3 – 2.9 \times 10^5$ cps	<3 nW after	5 – 7 nW before <1.5 nW after	NA	NA
Signal (O_2)	$1.6 – 1.8 \times 10^5$ cps (room temp)	~2.3 nW	0.9±0.2nW all temps	NA	NA
Measurement System	SPEX Fluorometer ~32°	Fiber system NA=0.22 13°	Fiber system NA=0.22 13°	NA	NA
Effective Sensor Area	30 mm^2	0.25π mm^2 fiber: FP-1.0-UHT	0.25π mm^2 fiber: FP-1.0-UHT	NA	NA

Good adhesion to the substrate surface is one of the most important requirements of any successful sensor based on sol-gel films. The surface of glass is typically terminated with silanol groups that participate in sol-gel reactions leading to excellent adhesion of the sol-gel film to the surface. The substrate surface, however, must be appropriately prepared, and be free of all organic contaminants. Achieving good adhesion to flat substrates is relatively simple when the substrate is borosilicate glass and is slightly more difficult with planar silica fused silica substrates. For fibers, two added complications are that the fiber is encased in several layers of organic polymers, each which must be completely removed to reveal the bare fiber. In the case of high temperature fibers, the cladding is a fluorine-doped fused silica glass. Shown in **Figure 10** are cross-sectional diagrams of the fibers used in this research. Although the 3M fibers are not designed for high temperature operation, their composition mimics that of the high temperature fibers so they were used for initial tests of the sol-gel film adhesion. The jacket and clapping of fibers are removed mechanically, and then a good solvent for the cladding is used to remove any residue of the cladding from the fiber. Once the silica fiber is exposed, the surface preparation mirrors that used for cleaning and conditioning planar substrates. Fibers were handed-dipped and then allowed to dry at to 70° C. The deposited films have reasonable mechanical stability and usually survive light tapping of the fiber tip on a hard surface or accidental dropping of the fiber on the floor. However, micrographs of the fibers show that the films are cracked and irregular (see fiber **E** in **Figure 8**), indicating that the adhesion of the composite to the fiber needs to be improved. More vigorous mechanical tests such as challenging the composite with adhesive tape usually remove the composite from the fiber. Since the fiber should be terminated in the same silanols as planar silica substrates, these results suggest that the cleaning procedure may not fully remove all organic species from the surface. We are currently testing the use of a simple UV/ozone treatment to remove residual organic residues from the exposed silica fiber.

1. CeramOptec 400°C fiber
part number: UV 600/660 P

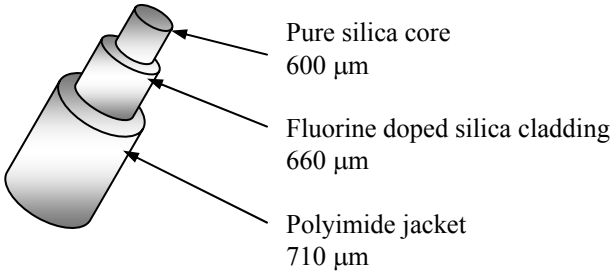

2. Fiberguide 200°C fiber
part number: SFS1000/1100z

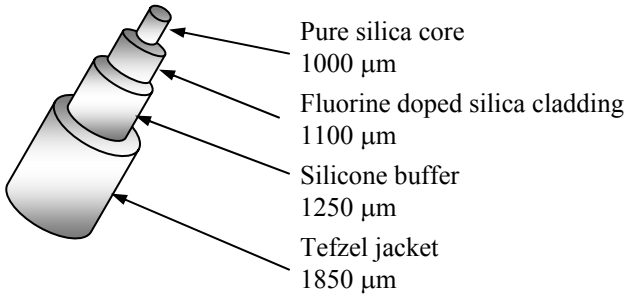

3. 3M fiber
part number FG-910-UER

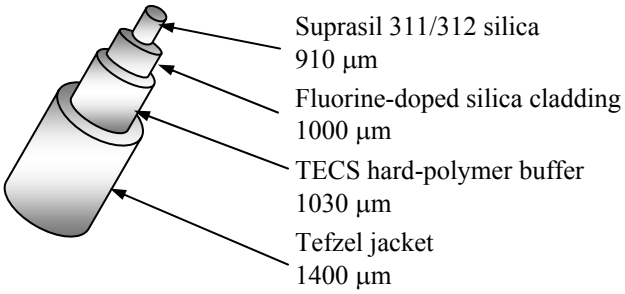

4. 3M fiber
part number FT-1.0UMT

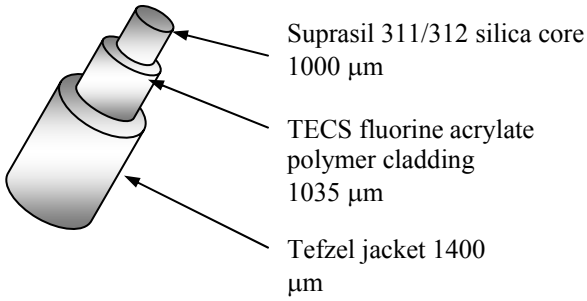

5. 3M fiber
part number: FP-1.0UHT

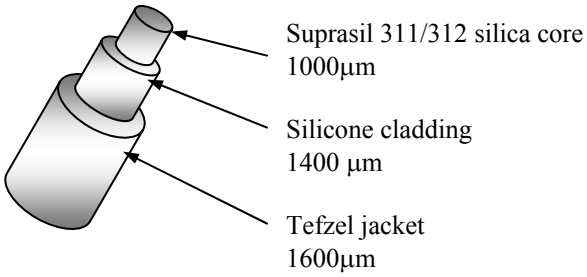

***Figure 10*:** Specifications of the optical fibers used for oxygen fiber sensor fabrication and testing the mechanical properties of the sol-gel films.

High temperature sensor measurements from fiber D - $K_2Mo_6Cl_{14}$ cluster containing sol-gel composite.

During this quarter we have demonstrated oxygen quenching from a fiber sensor up to 175 °C using the composite technique of embedding the molybdenum-containing sol-gel particles in an optically inactive binder. A tantalizing result of these measurements is that a thick film of the cluster containing composite on the tip of an optical fiber, displays a stronger degree of luminescence quenching at room temperature following high temperature cycling than any of our previous cluster containing planar substrates. We are investigating the mechanisms responsible for this behavior to take advantage of the enhanced luminescence intensity and oxygen permeability of these films.

The experimental geometry for the fiber sensor measurements is shown in **Figure 4**. Using a 365 nm LED (Nichia) light we launch 250 µW of pump power into the near end of a 1000 µm UV transparent fiber (3M FP-1.0-UHT). The UV light excites the clusters in the sol-gel composite at the tip on the far end of a ~15 cm long optical fiber. The fluorescence then returns through the optical fiber to a high sensitivity PMT (Hamamatsu R955) detector after passing through an objective lens and a dichroic beam splitter. Optical measurements were made with the sensor tip inside a flow-through gas chamber that could be heated to 400˚C. The spatial profile of the temperature distribution around the sensor tip was measured to be 4 °C within of 8 mm of the tip. The repeatability of measuring the temperature at the original tip position is approximately 0.8 °C, giving us an error of about 1 °C in our thermometry. The stray light intensity in our experiment is around 0.14 nW with an additional 0.07 nW due to scattering from the front and back face of the fiber.

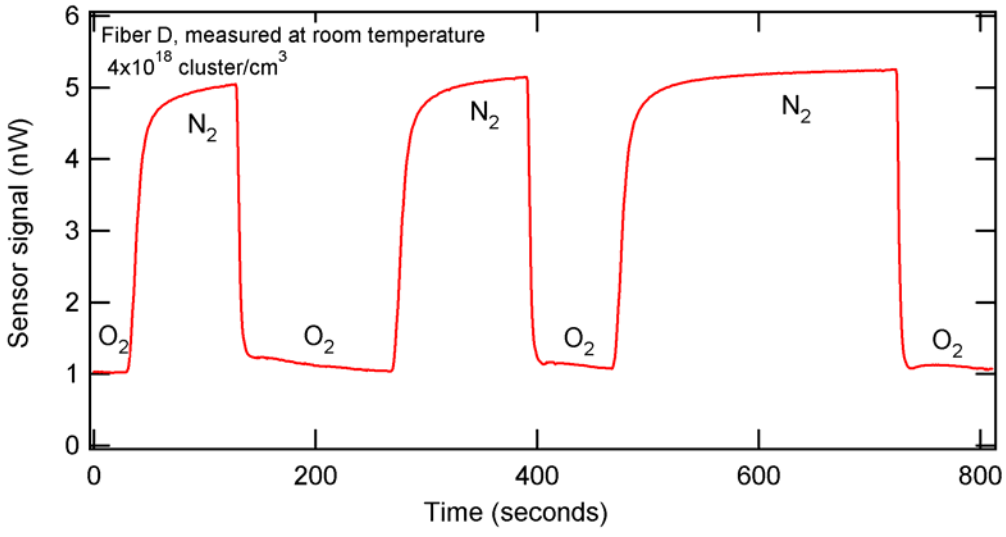

***Figure 11*:** Oxygen quenching at room temperature for fiber D, prior to thermal cycling.

All the measurements in this section were made on a single fiber sensor (Fiber D) fabricated by dip coating (thickness 200µm) a powdered sol-gel/cluster and sol-gel solution binder on a 1000 µm diameter fiber (3M FP-1.0-UMT). After aging for about

two days in air and curing for 12 hours in air at 70 °C, the room temperature quenching ratio of the sensor is 5.2 ± 0.5, see **Figure 11**. This result is higher than the typical quenching ratio of ~4X that we obtained from the planar sol-gel films. Interestingly the quenching ratio from this thick film was twice that of slide 38Q, (film thickness <1μm, quenching ratio 1.9 ±0.5) which was processed with a similar sol-gel/cluster blend. The stronger luminescence signal of thicker films allows a more accurate measurement of the luminescence intensity in 22% O_2, and the difference in quenching ratios for nominally identical films may simply reflect a more precise determination of the quenching ratio. There are however differences in the processing between Fiber D and slide 38Q, and thus we cannot discount the possibility is that the thicker film has a higher permeability due to unknown structural differences. First, the sol-gel binder used for slide 38Q contained molybdenum clusters that had not been aged or thermally cycled, whereas the binder for Fiber D had no clusters. Secondly, slide 38Q was cured for 30 minutes at 200 °C, whereas Fiber D was cured for 12 hours at 70 °C. We are investigating the mechanisms responsible for the enhanced room temperature quenching following thermally cycling of the thick films.

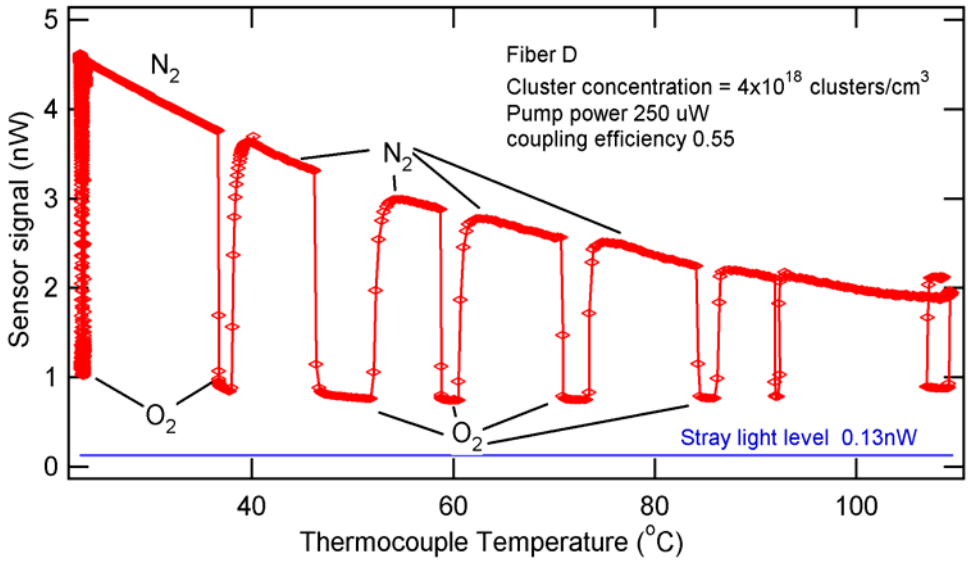

***Figure 12*:** Luminescence intensity and oxygen quenching as a function of temperature for fiber optical sensor fiber D (MM5-based composite). While heating, the gas in the chamber was switched between 99.999% N_2 to 21% O_2. These measurements were made in a high temperature gas chamber (25 mL) at a flow rate of 1.5 L/min. The lumophore concentration is approximately (4.8 ± 0.5) $\times 10^{18}$ clusters/cm^3.

Real-time measurements of the luminescence intensity of Fiber D as a function of thermocouple temperature while switching between 100% N_2 and 21% O_2 are given in **Figure 12** during a heating cycle from room temperature to 110 °C and in **Figure 13** while cooling from 175 °C to 30 °C**.** Quenching ratios (ratio of signal in 99.999% N_2 vs 21% O_2) of 2.4X and (1.3 ± 0.2)X were obtained at 115 °C and 175 °C respectively, demonstrating high temperature fiber operation. Two additional observations indicate

that using pulverized cluster containing sol-gel particles in an optically inert binder has positive consequences in terms of oxygen permeability of the composite and survivability of the cluster luminescence following high temperature cycling. First, the magnitude of the luminescence signal in nitrogen at 115 °C and 175 °C respectively is only 3.2 dB and 7 dB lower than the room temperature value. These light levels are well within our current experimental floor of around 0.21 nW. Secondly, the quenching ratio at room temperature actually *increases* slightly from the initially value of (5.2 ±0.5)X to >6X following both heat cycles. This is a very encouraging result as our previous heat cycling experiments on Mo cluster directly imbedded in a sol-gel film (in a planar geometry) had all suffered from a severe degradation of the oxygen permeability after heat cycling. We are investigating potential mechanisms. A possible explanation is that the pulverized particles are relatively insensitive to thermal cycling as they were obtained from a preformed and fully equilibrated cluster containing sol-gel matrix. In addition the optically inactive binder may be contracting during thermal cycling, thereby increasing the oxygen permeability of the composite.

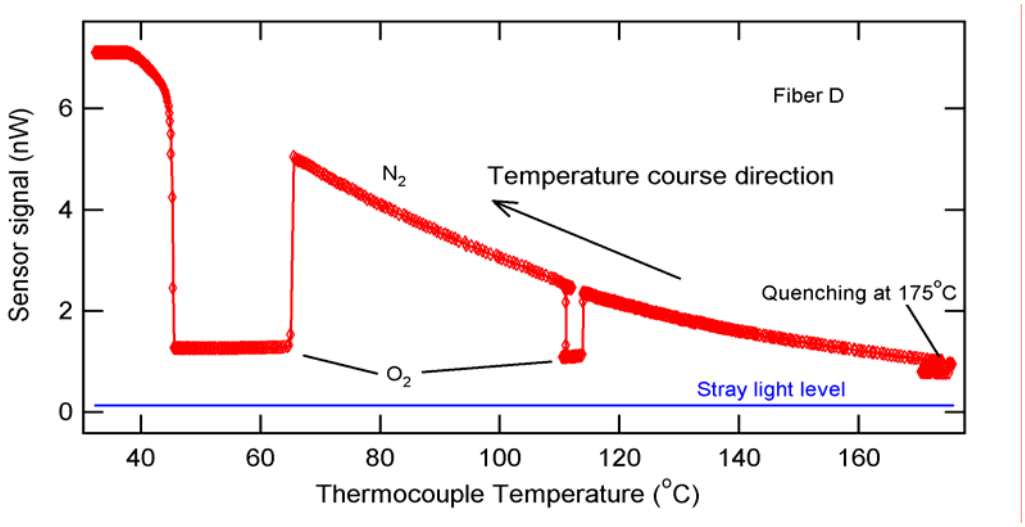

Figure 13: High temperature fiber sensor and oxygen quenching data for Fiber D (see Figure 12 for details). Here we demonstrate oxygen quenching of 1.3 ± 0.2 at 175 °C.

Note that although the fiber used for making this sensor (3M FP-1.0-UHT) is rated for operation only up to 150 °C, by removing the silicone cladding, and letting the air in the surrounding act as the effective cladding, we were able to make measurements at higher temperatures. We are currently in the process of fabricating fiber sensors similar to Fiber D on our two high temperature fibers from Fiberguide and CermOptec. Table 3 lists the relevant properties of the various fibers we have been using for our experiments.

***Table 3*:** Calculated performance of four different high temperature optical fibers (1, 2, 4 and 5) compared to the fiber used (3) for our previous room temperature optical fiber oxygen sensor [5]. The signal for the other fibers are calculated relative that of fiber 1. From a 100 μm thick polymer/cluster composite immobilized on fiber 3, we obtained room temperature signals of 1 nW and 7.5 nW in 21% O_2 and pure N_2 respectively.

Fiber	Core Diameter (μm)	NA	Operating temperature (°C)	Relative sensor signal* (calculated)	Jacket diameter (μm)	Cladding diameter (μm)	Source part number
1	600	0.22	400	0.088	Polyimide 710	660	Ceramoptec UV600/660P
2	1000	0.22	200	0.25	Tefzel 1850	1100/1250	Fiber Guide SFS1000/1100Z
3	1500	0.39	125	1.0	Tefzel 2000	1550	3M FT-1.5-UMT#
4	1000	0.4	150	0.45	Tefzel 1600	1400	3M FP-1.0UHT#
5	910	0.22	125	0.20	Tefzel 1400	1000/1035	3M FG-910-UER#

*Assuming a 100 μm thick sol-gel/cluster composite on the tip of the fiber with 2.9 x 10^{19} clusters/cm^3 [5]

Silica core has a high $[OH]^-$ for improved UV transmission

The performance of fibers 1,2, 4, and 5 were calculated with the following assumptions:

(i) all clusters in a film of thickness t emit fluorescent photons into 4 π steradians
(ii) of these photons, NA/4π are collected by the fiber
(iii) the quantum yield of $K_2Mo_6Cl_{14}$ is the same as Mo_6Cl_{12}.
(iv) the pumping and collection efficiencies of the current setup (**Figure 4**) are the same as in [5]

We used the 3M fibers for sensor operating at lower temperatures (125 – 150 °C) and will use the Ceramoptec and Fiberguide fibers for higher temperature applications. The 3M and Fiberguide optical fibers have Suprasil cores, a high purity synthetic fused silica manufactured by flame hydrolysis of $SiCl_4$. Suprasil offers two advantages for UV fiber sensor operation. First, Suprasil has a high optical transmission in the ultra violet due to the sub-ppm level of transition material impurities. No fluorescence is observed below 254 nm, when using a 75 W low pressure Hg lamp for inspection. Secondly, Suprasil has minimum Raman and Raleigh scattering [8], due to the high degree of index homogeneity

that can be achieved either in one direction (the direction of use or functional direction) or all three dimensions. Note that the two high temperature fibers CeramOptec and Fiberguide, and the 3M FG series fibers of **Figure 10**, have fluorine-doped silica claddings which may effect the adhesion of the cluster containing sol-gel composite. The silicone-clad FP series from 3M is a large diameter UV fiber which was used as a low cost alternative for initial experiments up to 150 °C or 175 °C (after removal of the cladding).

High temperature survivability of spray coated $K_2Mo_6Cl_{14}$/sol-gel film (film 38Q)

We measured the optical properties of sol-gel films embedded with $K_2Mo_6Cl_{14}$ after they were subjected to heating protocols where both temperature and time were varied. We used the measured luminescence intensity of the film in nitrogen and its quenching in oxygen as an indication of the high temperature survivability of each film. The film was fabricated by our new composite material approach, which consists of embedding Mo-clusters/sol-gel particles in a binder to improve film porosity in high temperature. This potassium-salt/sol-gel film slide (38Q) was prepared by spray coating using the procedure described in the experimental and heated for 30 minutes at 200 °C. Optical measurements of 38Q were taken 60 days after curing in air at room temperature. In contrast with Fiber D, which was made from the same Mo-cluster/sol-gel particles, the binder used in this case did contain optically active Mo-cluster.

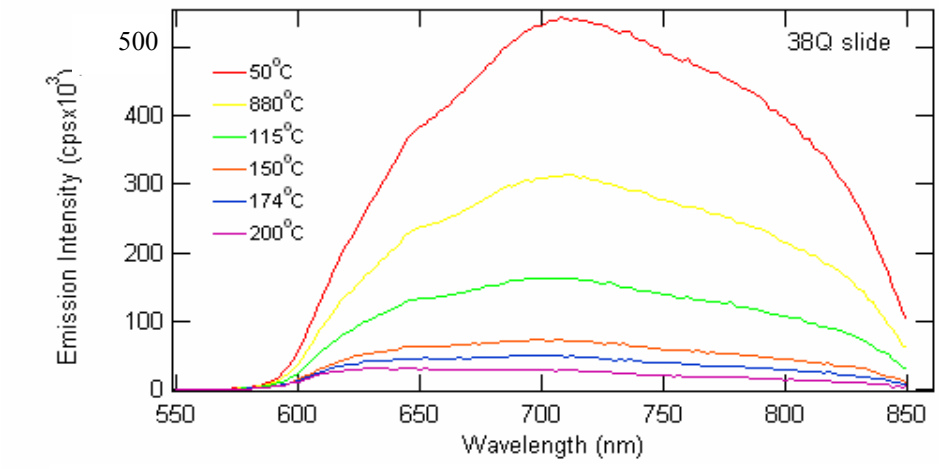

Figure 14: Thermal dependence of the emission spectra for film 38Q cured at 200 °C for 30 minutes. The emission intensity is a function of temperature, but the line-shape is temperature independent. All spectra were sampled in 99.999% nitrogen environments. The cluster source was MM8 and the film concentration is $(5\pm1.1) \times 10^{20}$ clusters/cm^3 based on an estimated film thickness of (700 ± 300) nm.

In-situ measurements of the emission spectra of film 38Q, prepared from potassium salt MM8, from 50 to 200 °C are shown in **Figure 14**. These are the first measurements we have been able to obtain free of fluorescence from the heating structure itself. The

backside of the quartz substrate was heated locally in only the area of the pump beam (2 × 10 mm) using a Si substrate / Pt heater sandwich. The "sandwich" structure is held in intimate contact with the quartz substrate without the use of any adhesives in the region to be probed to circumvent problems due to fluorescence from the Ag paint and the Pt heater itself. The high thermal conductivity of Si allows for uniform and rapid heating of the area of interest. We measured the emission spectra at different temperatures. After subtracting the contribution of Raman scattering from the sol-gel matrix, only minor changes in the line-shape were observed confirming that sol-gel immobilization and thermal cycling did not adversely affect the emission from the potassium salt (MM8).

Shown in **Figure 15** are time dependent measurements (time base acquisition or TBA, Fluorolog-3) of the emission intensity at 674 nm while alternating between 99.999% nitrogen and 20.7% oxygen. The data indicate fast oxygen quenching as each point represents a 0.5 second time interval. The luminescence intensity decreases with temperature, but the quenching ratio defined as the ratio of the luminescence in 99.999% N_2 versus to that in 20.7% O_2 remains approximately constant but low (1.3) at 200 °C.

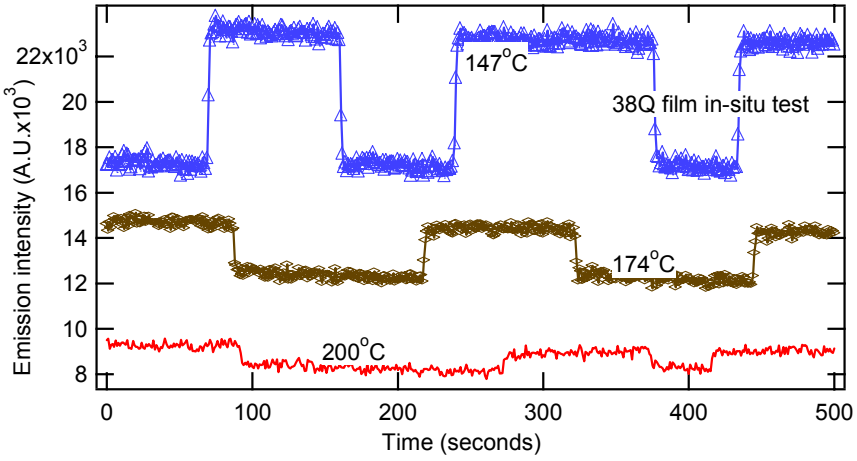

***Figure 15*:** Time dependent quenching measurements at 674 nm of sol-gel film 38Q alternating between a 99.999% N_2 and 20.7% O_2 gas environment at 147°C, 174°C and 200°C. The response time of the film is fast, ≤ 1 second. The film was pumped at 313 nm.

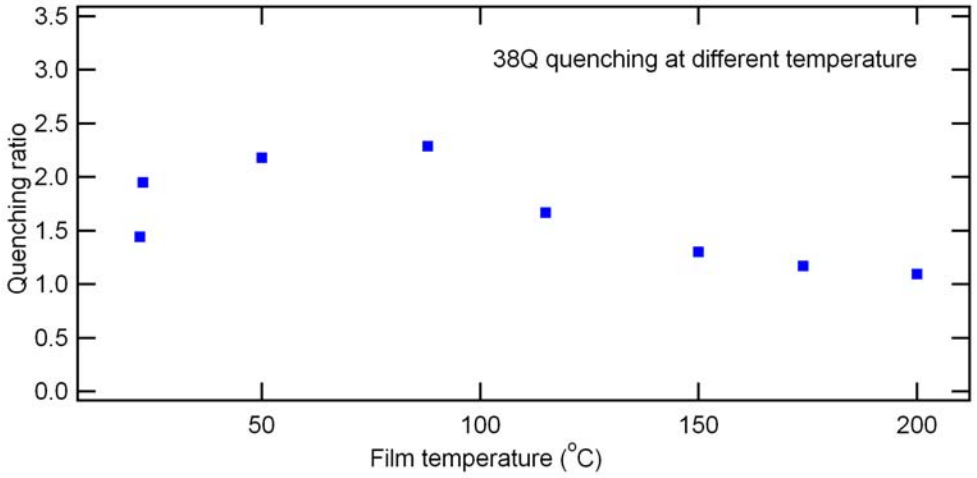

***Figure 16*: Quenching ratio as a function of film temperature for sol-gel film 38Q derived from the time dependent measurements of Figure 15. The quenching ratios are relatively independent of temperature, but the magnitude itself is small.**

The oxygen quenching ratio over the entire operational temperature range is shown in **Figure 16**. The initial quenching ratio at room temperature is approximately 1.5X, increasing ~2.3X at 100 °C. In addition to these measurements, we monitored the oxygen quenching ratio following thermal cycling up to 200 °C, (see **Figure 17)**, to determine the stability of the optical characteristics of the cluster luminescence. The average value of the quenching ratio was 1.6X with variations of ~ 30% around this value. The intensity of luminescence is repeatable to within 5%.

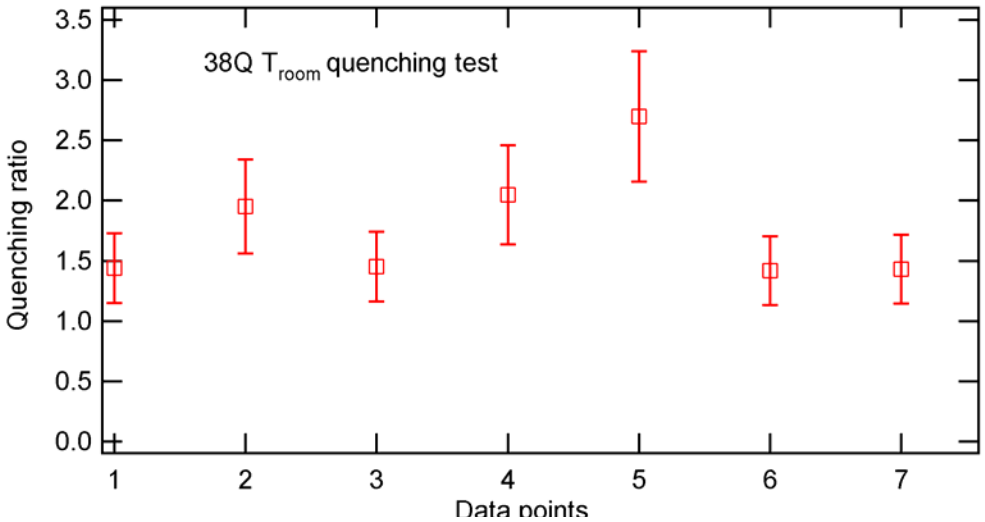

Figure 17: Demonstration that the room temperature quenching ratio of slide 38Q is relatively unaffected by temperature cycling; measurements from the (1) first day, (2) one day later, following cycling to: (3) 50 °C, (4) 88 °C, (5) 115 °C, (6) 150 °C and (7) 200 °C. The lowest value obtained is 1.45X.

The results from Film 38Q show that the optical properties of the film are stable even after various long term heating protocol and the oxygen permeability of the composite is not degraded by temperature cycling. This is a first for our Mo-containing sol-gel films. As we have discussed in our previous reports, the permeability of sol-gel matrices is related to the free volume within the matrix and is highly dependent on the details of the synthetic parameters used to prepare the sol-gel matrix cell gel. Briefly, a sol-gel synthesis involves the acid or base catalyzed hydrolysis and condensation of metal alkoxides such as tetraethylorthosilicate. As the reaction proceeds to completion the sol-gel solution is converted to a continuous solid matrix. If spectator compounds are present, in our case $K_2Mo_6Cl_{14}$, they are entrapped within the matrix. Essentially all sol-gel films densify to some extent as they cure and further densify after drying at high temperatures. In the composite approach, the $K_2Mo_6Cl_{14}$ is embedded in a sol-gel matrix that has been fully cured. Thus, no further evolution of sol-gel matrix occurs during measurements at high temperature and the permeability and quenching characteristics of the composites are stable. In principle, evolution of the *binder* could decrease the permeability and reduce the quenching ratio of the composite, but the experimental data to date indicate no deleterious effects from the binder.

In this section we have shown the promising results from planar films prepared from powder sol-gel solutions. The results corroborate one of the potential advantages we had identified for the composite approach – that it would likely lead to fiber sensors that had stable and predictable optical properties. Preliminary measurements of high quenching ratios for fibers sensors prepared by the composite route suggests a physical model where the cluster-containing particles form a continuous porous network analogous to a scintered glass, highly permeable but mechanically and thermally stable. We plan to examine the structure more closely to understand and improve sensor performance.

CONCLUSIONS

In our previous report, we proposed a composite approach to overcome the problems of poor long-term stability at 200 °C and low oxygen quenching ratios in sol-gel films containing luminescent $K_2Mo_6Cl_{14}$ clusters. Using slurries made from cured $K_2Mo_6Cl_{14}$/sol-gel nanoparticles in a pure sol-gel binder, we successfully spray-coated and dip-coated the tips of fibers as well as planar substrates. Optical fiber sensors prepared from 50 and 60 w/w% cured $K_2Mo_6Cl_{14}$/sol-gel nanoparticles show increased thickness, adhesion, oxygen quenching, and the required lumophore concentration for an optical fiber based oxygen sensor. An exciting result of our fiber measurements is that the 200 μm thick film displays a stronger degree of luminescence quenching by oxygen after high temperature cycling than any of our previous films. This indicates that the composite retains its oxygen permeability following thermal cycling.

We have designed and built a compact high temperature fiber sensor test setup to characterize devices up to 350 °C in a gas flow through system. The setup is designed to be portable for field testing and uses an inexpensive, ~$6.00 UV light emitting diode as the excitation source. A data acquisition system has been developed to simultaneously record the sensor luminescence signal and sensor temperature, to ±1 °C. We expect to be able to determine the sensor response time to better than 10 s, as the gas exchange time in the chamber is <6 s for a 1.5 L/min flow. Using this system, we characterized the luminescence signal from a fiber sensor (Fiber D) fabricated using the composite approach of embedding cured $K_2Mo_6Cl_{14}$/sol-gel nanoparticles in an optically inert sol-gel binder was measured from room temperature to 175 °C. Quenching ratios (signal in pure N_2 vs 21% O_2) of 2.4X and 1.3X were obtained at 115 and 175 °C respectively. The signal to noise ratio for the 115 °C measurement is ~4dB in oxygen. We are in the process of reducing the background light level of our present setup below 0.22 nW to improve our sensitivity.

In addition to the fiber sensor experiments we performed *in-situ* measurements of the emission spectra of a composite film deposited on a planar substrate (Film 38Q) up to 200 °C. This is the first high temperature data we have been able to obtain that is free of fluorescence generated by the heating structure itself. The spectra show that the emission line shape remains relatively constant as a function of temperature. By monitoring the emission intensity as a function of time, while alternating between pure nitrogen and 21% oxygen, we find a quenching ratio of about 1.3X at 200 °C. The response time of this film is remarkable fast <2.5 s at 175 °C. The sensor signal switches between two discrete levels, without any of the long term exponential tails observed in our previous sol-gel films.

Research Timetable

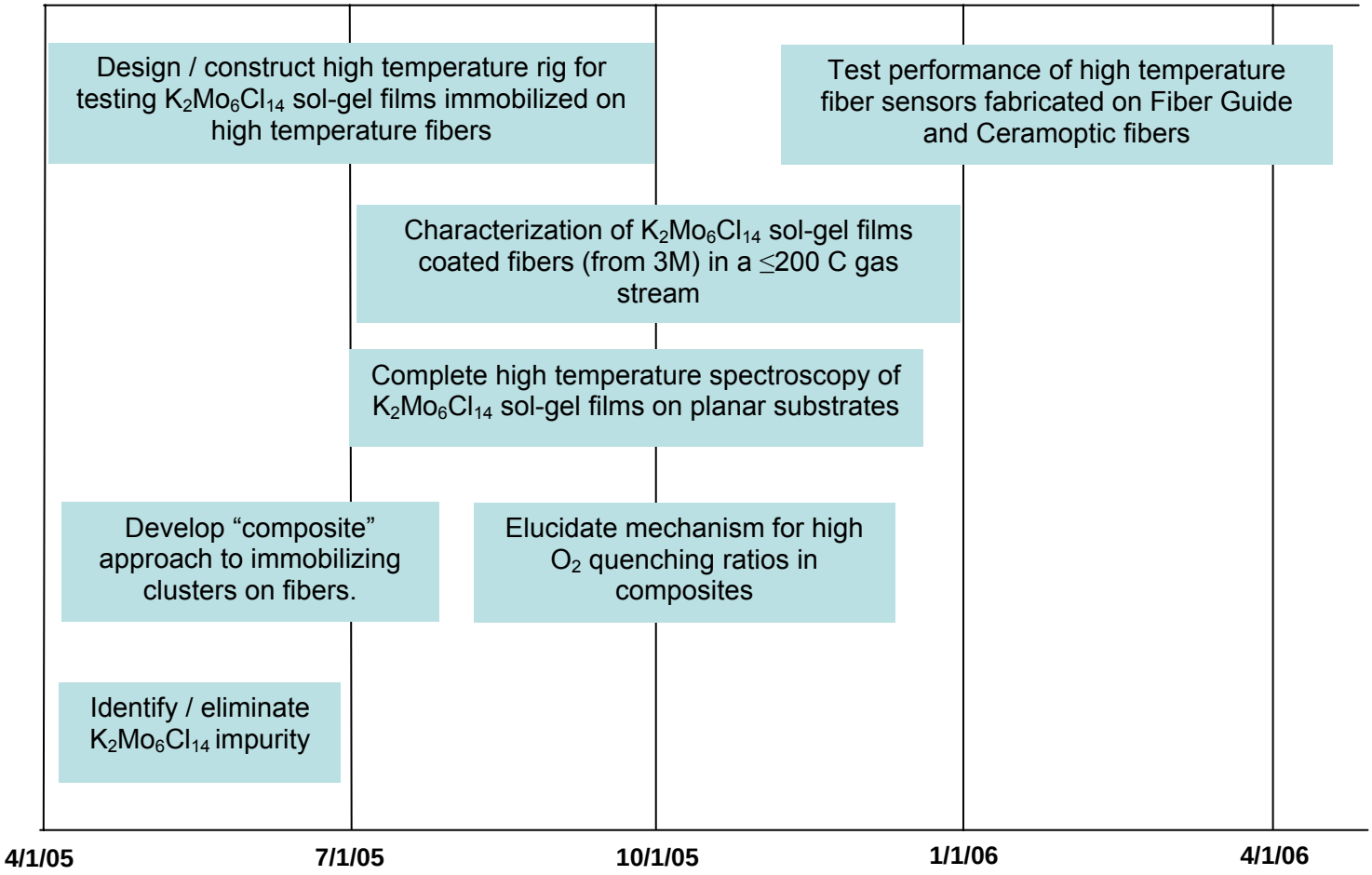

REFERENCES

[1] R. D. Mussell, Ph. D. thesis, Michigan State University (East Lansing), **1988**.
[2] M. D. Newsham, Michigan State University (East Lansing), **1988**.
[3] M. D. Newsham, M. K. Cerreta, K. A. Berglund, D. G. Nocera, *Mater. Res. Soc. Symp. Proc.* **1988**, *121*, 627.
[4] C. J. Ruud, Ph. D. thesis, Michigan State University (East Lansing), **1999**.
[5] R. N. Ghosh, G. L. Baker, C. Ruud, D. G. Nocera, *Appl. Phys. Lett.* **1999**, *75*, 2885.
[6] J. T. Remillard, J. R. Jones, B. D. Poindexter, C. K. Narula, W. H. Weber, *Appl. Opt.* **1999**, *38*, 5306.
[7] http://www.alltronics.com/download/R955.pdf
[8] Max Born and Emil Wolf, 7th edit, *Principles of Optics*

BIBLIOGRAPHY

None.

LIST OF ACRONYMS AND ABBREVIATIONS

HCl – Hydrochloric Acid
MeOH – Methanol
CH_3CN – Acetonitrile
TEOS – Tetraethyl orthosilicate

APPENDIX A - ACKNOWLEDGEMENTS

We wish to acknowledge the contribution of Reza Loloee, Michigan State University, in developing the high temperature sensor characterization system.